Analysis of the human arm gesture for optimizing cutting process in ham deboning with a redundant robotic cell

Kévin Subrin, Laurent Sabourin, Franck Stephan, Grigoré Gogu, Matthieu Alric, Youcef Mezouar

Analysis of the human arm gesture for optimizing cutting process in ham deboning with a redundant robotic cell

Kévin Subrin, Laurent Sabourin, Franck Stephan and Grigoré Gogu
Pascal Institute – Machines, Mechanisms and Industrial Systems Group,
French Institute for Advanced Mechanics/Blaise Pascal University/CNRS, Clermont-Ferrand, France

Matthieu Alric
Pre-Engineering – Mechanical and Robotic Design, ADIV – Meat Performances, Clermont-Ferrand, France, and

Youcef Mezouar
Image, Perception Systems and Robotics, French Institute for Advanced Mechanics/Blaise Pascal University/CNRS, Clermont-Ferrand, France

Abstract

Purpose – The mechanization of the meat cutting companies has become essential due to the lack of skilled workers and to working conditions. This paper deals with the analysis of human gestures in order to improve the performance of a redundant robotic cell. The aim is to define optimization criteria linked to the process and the human gesture analysis to improve the cutting process with a redundant robotic cell. Design/methodology/approach – This paper deals with an optimized path planning of complex tasks based on the human arm analysis. The first part details the operator's manual work. The robotized cutting strategy using bones as a guide associated with an industrial force control leads to the tasks redefinition. Thus, the analysis of the arm during the tasks is presented. With a robotic model, the authors evaluate the relevance of two criteria (kinematic and mechanical) that the operator naturally manages. These criteria are used to improve the robotized cutting process by using redundancy. Simulation work and experimentation are presented to show the enhanced performance.
Findings – The paper explains how to define optimization criteria based on human arm analysis to realize cutting operations which require force or dexterity performance. It presents a study on the criteria weighting on a robotic arm model established through human arm analysis. The optimized cutting process clearly shows improvement.
Research limitations/implications – The scalability of the ham implied the definition of iterative trajectories to follow the curvature of the bone. Due to the use of an industrial force control, no online optimization can be achieved. The off-line optimization implies that the boundary of the trajectory space is technically feasible. Nevertheless, more information has to be extracted from the deboning process such as vision data in order to improve cutting quality. Practical implications – This study was carried out within the framework of several national and European projects (FUI SRDViand, ANR ARMS, FP7 Echord Dexdeb) in collaboration with ADIV (Meat Institute Development Agency). The redundant robotic cell was developed and implemented at ADIV and used for feasibility studies in connection with SME/SMI French sector.
Originality/value – The paper deals with the cutting of soft bodies such as meat and complex human gesture analysis, which constitute an innovative challenge for the coming years in order to help or replace humans in industrial meat companies with difficult working conditions.

Keywords Gradient projection method, Human gesture analysis, Meat cutting, Offline programming, Path planning, Redundancy

Introduction

The meat industry is looking for reliable robotic solutions to decrease the difficulty and danger of cutting and deboning operations. The unattractiveness of these jobs is explained by difficult working conditions (cold, unsocial hours) and a number of diseases related to musculoskeletal disorders (MSDs) and accidents (CNAMTS, 2004). Some countries such as Denmark (DMRI) (Hinrichsen, 2010), New Zealand (MIRINZ) (Aimers *et al.*, 2003) and Japan with *Hamdas R* (Kusuda, 2010; Hamdas, 2010) have already started robotizing meat processing. The first part of this paper presents constraints associated with meat cutting taking as an example ham deboning. This work leads to the implementation of a redundant robotic cell combining an industrial robot with a turntable allowing for access to various operations. The second part focuses on the analysis of the human arm gesture where

The authors acknowledge the financial support for this work in the framework of InnovaPole Project funded by Region Council of Auvergne and FEDER, European Project ECHORD-DEXDEB and Project ANR-ARMS.

two criteria based on dexterity and mechanical performance are deeply explained. The third part presents the path planning for the redundant robotic cell, setting criteria and their weightings. Finally, the last part deals with the experimentation and the results in the frame of ham deboning to show the performance of the proposed approach to improve the cutting process.

1. Ham deboning process

We first present the manual ham deboning operations, their complexity and the constraints to robotize such operations (James *et al.*, 2009). These constraints led us to consider the whole process to define a strategy for robotic deboning.

1.1 Manual ham deboning

Ham deboning is a complex process associated with a set of anatomical cuttings which require expertise acquired through specific training. These cuttings introduce a set of constraints on the redefinition process:

- *Variability.* Even if the hams are each calibrated to 2 kgs, the percentage of fat and muscle texture varies depending on the animal and maturation.
- *Cutting on deformable bodies.* The forces applied and successive cuts imply a distortion of the muscles that requires self adapting trajectories.
- *Sensory coupling.* The skilled operator uses a permanent coupling between vision and perceived forces during cutting, associated with the anatomical memory of the operator.

The scenario of the robotic deboning process requires the main steps to be the definition of strategies and the sequence of operations (Figure 1). These have previously been manually tested to validate the technical feasibility, quality of cutting and material yield, as applied to ham deboning. The ham is positioned vertically and maintained on the upper side of the femur head and on the bottom part of the shank. This allows to benefit from gravity in order to facilitate the separation of bones and muscles. The whole handling system (Figure 2(c)) is synchronized in rotation with the robot (Figure 2(d)) to facilitate access for the various steps of cutting operations. In the rest of this paper, we will only be dealing with the complex cutting operations for opening ham (Figure 2(a) and (b)).

1.2 Cutting strategies using the bone as a guide

The cutting strategies include the use of an industrial force control (ABB, 2005) and a characterization study to evaluate the blade behaviour during the cutting. In fact, the force sensor is fixed between the robot and the tool to detect the interface between the meat and the bones. The path is constructed iteratively, where each set is bounded by a security zone to limit the robot's deviation. The control is similar to an external hybrid force control (Perdereau and Drouin, 1993). The working principle consists in a force variation due to a contact between the robot and its external environment which is converted to a variation of displacement. Moreover, in order to improve the cutting quality, experimental study (Guire *et al.*, 2010) evaluated the parameters α, V_f, V_n and F_c to analyse their influence (Figure 3). The study showed a significant reduction of force F_c and good cutting if α is close to 30° and/or V_n is non null. We focus on two cuttings with different constraints, AB cutting which requires the application of a strong F_c cutting force and BC cutting associated with trimming the kneecap which requires dexterity (Figure 2(a) and (b)).

2. Human arm gesture

The human arm is a redundant architecture and many authors work on the analysis of the gesture to understand how humans optimize their movements to perform complex tasks (Campos and Calado, 2009). The literature presents models with seven DoFs (Artemiadis *et al.*, 2010a, b; Kim *et al.*, 2012). However, due to the complexity of this architecture, the authors simplify it to a non redundant architecture depending on the task being studied (Artemiadis *et al.*, 2010a, b). The analysis of postures aims to understand the strategies and optimization performed by the human operator like arm stiffness (Gomi and Kawato, 1997) or kinetic energy (Debicki *et al.*, 2010). Nevertheless, contributions show that the study of stress fields is essential for understanding a gesture (Mussa Ivaldi *et al.*, 1985; Artemiadis *et al.*, 2010a). As part of our work, we seek to evaluate the effectiveness of dexterity criteria and mechanical performance (Artemiadis *et al.*, 2010b) by comparing the results of our path planning in relation with the human gesture.

2.1 Proposed human arm model

The cutting task dimension is six, so we defined a six DoFs model which consists in two DoFs at the shoulder, three DoFs at the elbow and one DoF at the wrist. We introduce two additional angles: θ_{tool} characterized by the orientation angle around the blade plane and $\theta_{shoulder}$ characterized by the orientation angle around y_0 (Figure 4). We propose to evaluate the ratio of speed and torque in order to understand which criteria must be used to optimize the robotic cell behaviour.

2.2 Criteria used for the human arm analysis

2.2.1 Dexterity criteria

This criterion is focused on expressing the kinematic performance of the effector to move in the d advance direction with the V_f speed reference. We adopt the approach proposed by Dubey (Dubey and Luh, 1988) which introduces the concept of manipulator velocity ratio (MRV), as the ratio between the operational speed and the joint speeds defined by:

$$\begin{aligned} &|\dot{x}|_{w_x} = \sqrt{\dot{x}^T W_x \dot{x}} \text{ and} \\ &|\dot{q}|_{w_q} = \sqrt{\dot{q}^T W_q \dot{q}} \text{ and } \dot{x}_v = W_x^{1/2}\dot{x} \text{ and } \dot{q}_v = W_q^{1/2}\dot{q} \end{aligned} \quad (1)$$

The matrices W_x and W_q, are positive definite weighting matrices which, for simplicity, are chosen diagonal. They help in distributing the relative influence of joint velocities and speeds of the effector. In our case, W_q is set using the joint maximum speeds to homogenize their influence. W_x is defined as the identity matrix without favoring any direction. In this form, we express the direct kinematic model using the Jacobian matrix $\mathcal{J}_v$ including joint maximum speeds by:

$$\begin{aligned} &\dot{x}_v = \mathcal{J}_v \dot{q}_v \text{ with } \mathcal{J}_v = W_x^{1/2} \mathcal{J} {W_q}^{1/2} \text{ and} \\ &W_q(i,i) = \frac{1}{\dot{q}_{i_{\max}}^2}, i = 1, \ldots, n \end{aligned} \quad (2)$$

By introducing the pseudo inverse matrix $\mathcal{J}_v^+ = \mathcal{J}_v^T \left(\mathcal{J}_v \mathcal{J}_v^T\right)^{-1}$ (Moore Penrose) in the expression of r_v speed ratio together with the unit vector u_v along $\dot{x}_v$, we obtain the expression of the ratio:

Figure 1 (a) Opening following the second fat vein, (b) cut along the shank, (c) extraction of the femur, (d) extraction of the patella, tibia and fibula

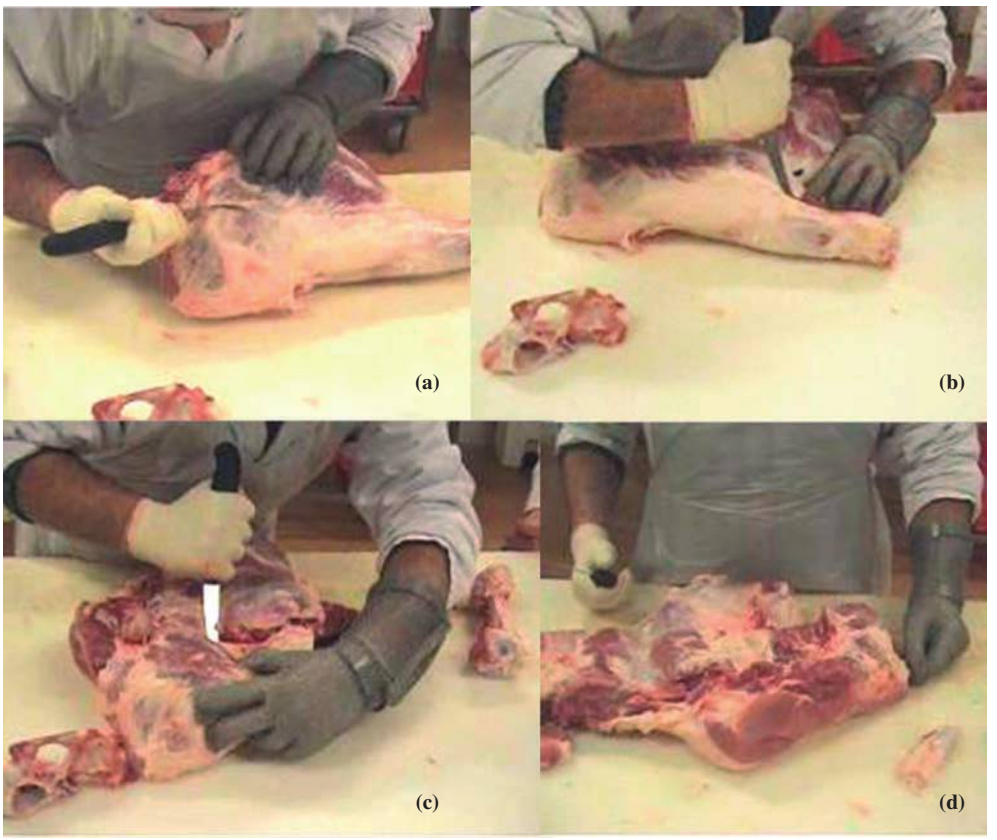

$$r_v = \frac{|\dot{x}|_{w_x}}{|\dot{q}|_{w_q}} = \sqrt{\frac{\dot{x}_v^T \dot{x}_v}{\dot{q}_v^T \dot{q}_v}} = \sqrt{\frac{\dot{x}_v^T \dot{x}_v}{\left(\mathcal{J}_v^+ \dot{x}_v\right)^T \mathcal{J}_v^+ \dot{x}_v}} = \frac{1}{\sqrt{u_v^T \left(\mathcal{J}_v \mathcal{J}_v^T\right)^{-1} u_v}} \text{ with } u_v = \frac{\dot{x}_v}{\sqrt{\dot{x}_v^T \dot{x}_v}} \tag{3}$$

This permits to define a kinematic criteria by:

$$\Phi_v(q) = u_v^T \left(\mathcal{J}_v \mathcal{J}_v^T\right)^{-1} u_v \tag{4}$$

The decrease of this criterion $\Phi_v(q)$ reflects an increase in the speed ratio. However, its value cannot directly determine whether the cell is able of generating the V_f desired speed. This criterion is related to the norm of the speed vector; it does not take into account each axis separately. Considering that the variation in orientation of the effector remains low, the norm of the operational speed vector along the d direction is given by V_f. We then obtain:

$$\forall i \in [0, n], \left|\frac{\dot{q}_i}{\dot{q}_{i\max}}\right| \leq |\dot{q}|_{W_q} \text{ with } |\dot{q}|_{W_q} = |\dot{x}|_{W_q} \sqrt{\Phi_v(q)}$$
$$\text{where } \left|\frac{\dot{q}_i}{\dot{q}_{i\max}}\right| \leq V_f \sqrt{\Phi_v(q)} \tag{5}$$

In our development, we study the ability to achieve the r_{vd} desired kinematic ratio dealing with the joint speed which brings its maximum speed closer:

$$r_{vd} = \min_i \left(\left|\frac{\dot{q}_{i\max}}{\dot{q}_i}\right| \right) \text{ with } r_{vd} \geq 1 \tag{6}$$
$$\text{for a feasible trajectory}$$

Thus, the increase of the r_{vd} ratio reflects an increase in the V_f speed capacity along the d direction.

2.2.2 Mechanical performance criteria

This criterion is intended to express the mechanical performance of the effector to transmit a f force along the d' direction. We choose once again the approach proposed by Dubey and Luh (1988) which introduces the concept of manipulator mechanical advantage (MMA) as the ratio between the norm of f force in the operational space and the norm of the joint torques defined by:

$$|f|_{w_f} = \sqrt{f^T W_f f} \text{ and } |\tau|_{w_\tau} = \sqrt{\tau^T W_\tau \tau} \text{ and } f_m = W_f^{1/2} f \text{ and } \tau_m = W_x^{1/2} \tau \tag{7}$$

W_τ is defined using the maximum joint torques to homogenize the influence of the joint torques. W_f is defined as the identity matrix without favoring the force direction. In this way, we express the direct static model using the $\mathcal{J}_m$ weighted Jacobian matrix introducing the maximum joint torques by:

Figure 2 (a) Cutting operations in the robotic process, (b) real cutting to be realized, (c) ham support equipped with a force sensor on the upper clamp, (d) robotic cell for meat cutting

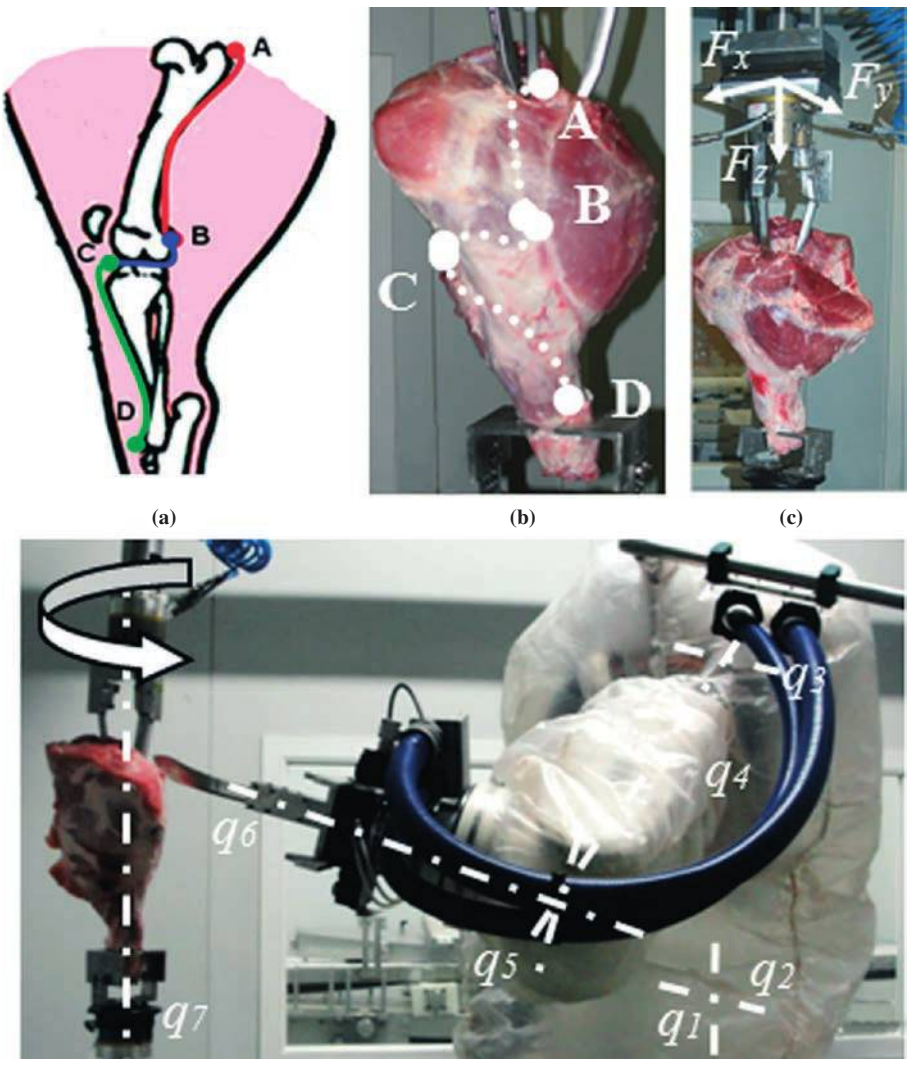

(a) (b) (c)

(d)

Figure 3 Establishing the cut to follow the shape of the bone in the cutting plane P_c

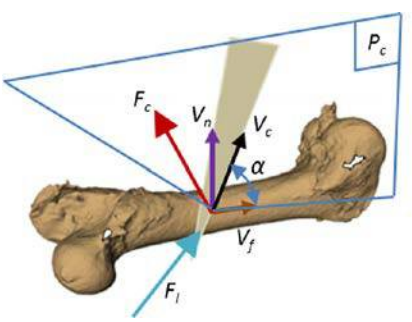

α	Cutting angle
F_c	Cutting force
F_l	Lateral force
V_c	Cutting speed
V_n	Normal speed
V_f	Advance speed

$$\tau_m = \mathcal{J}_m^T f_m \text{ with } \mathcal{J}_m = {W_f}^{1/2} \mathcal{J} W_\tau^{1/2} \quad \text{and } W_\tau(i,i) = \frac{1}{\tau_{i_{\max}}^2}, \; i = 1, \ldots, n \tag{8}$$

By introducing the Moore Penrose matrix $\mathcal{J}_m^+ = \mathcal{J}_m^T (\mathcal{J}_m \mathcal{J}_m^T)^{-1}$, we obtain the expression of the ratio:

$$r_m = \frac{|f|_{w_f}}{|\tau|_{w_\tau}} = \sqrt{\frac{f_m^T f_m}{\tau_m^T \tau_m}} = \sqrt{\frac{f_m^T f_m}{f_m^T \mathcal{J}_m \mathcal{J}_m^T f_m}} = \frac{1}{\sqrt{u_m^T (\mathcal{J}_m \mathcal{J}_m^T) u_m}} \text{ with } u_m = \frac{f_m}{\sqrt{f_m^T f_m}} \tag{9}$$

It permits to define the mechanical performance criteria as:

$$\Phi_m(q) = u_m^T (\mathcal{J}_m \mathcal{J}_m^T) u_m \tag{10}$$

Taking into account that the variation in orientation of the end effector is small, we obtain, as previously, the ratio of mechanical performance such that:

Figure 4 Proposed model of human arm – definition of the human arm joint angles $\theta_{ii\ 1}$

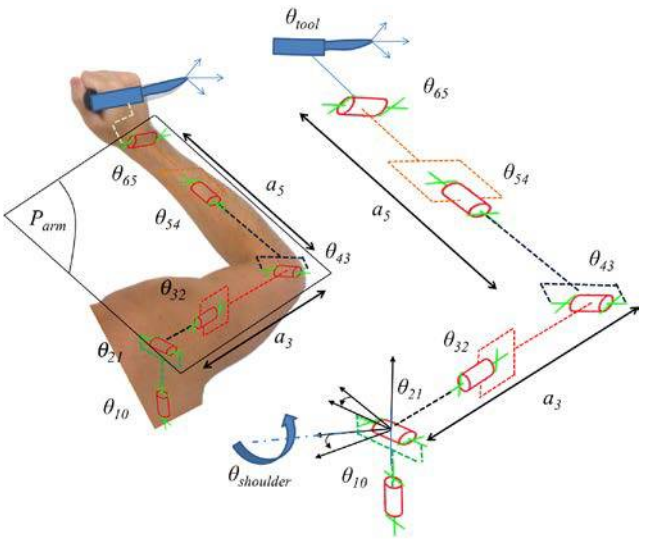

$$\forall i \in [0,n], \quad \left|\frac{\tau_i}{\tau_{i\max}}\right| \le |\tau|_{w_\tau} \quad \text{with} \quad |\tau|_{w_\tau} \quad |f|_{w_f}\sqrt{\Phi_m(q)}$$
$$\text{where} \quad \left|\frac{\tau_i}{\tau_{i\max}}\right| \le f_f\sqrt{\Phi_m(q)} \tag{11}$$

In our development, we study the ability to apply the f_f reference force by studying the r_{md} mechanical ratio dealing with the joint torque which brings its maximum torque closer:

$$r_{md} \quad \min_i\left(\left|\frac{\tau_{i\max}}{\tau_i}\right|\right) \tag{12}$$

Thus, the increase of the r_{md} ratio reflects an increase in the force transmission capacity along the d' direction. We propose to evaluate the relevance of these two criteria for the characterization of the operator's arm behaviour.

The weighting matrix diagonals W_q and W_τ include maximum speeds and torques of a human arm. According to the person's morphology, these values may vary (from single to double) according to the operator's acquired physical skills. The literature gives some orders of magnitude. Missing values are estimated based on the assumption that joint velocities are highest at wrist and joint torques highest at the shoulder (Table I).

3. Trajectory planning

The cutting path planning is based on the resolution of geometric and kinematic models of a seven DoFs redundant robotic cell with multicriteria optimization (Figure 1(d)). The ham deboning cell includes a six DoFs industrial robot, synchronized with a one DoF vertical turntable. The geometric model and the kinematic model are formalized with the TCS method (Gogu *et al.*, 1997). The model includes the movement's inversion of the overall system relative to the movement of the turntable. This is equivalent to positioning the observer on the turntable instead of positioning it on the frame as usual. The resolution of the IKM of a redundant robot is an under constrained problem which thus admits an infinite number of solutions.

3.1 Resolution method

The problem of following trajectories with a redundant architecture amounts to finding the parameters which satisfy various constraints related to the task, the configuration and the capability expected. The classical method consists in using the Moore Penrose inverse matrix $\mathcal{J}^+$ (Liegeois, 1977) using the general solution:

$$\dot{q} = \mathcal{J}^+\dot{x} + \alpha(I \quad \mathcal{J}^+\mathcal{J})\nabla\Phi \quad \text{with} \quad \nabla\Phi \text{ gradient of } \Phi(q) \tag{13}$$

where $\mathcal{J}^+ = \mathcal{J}^T(\mathcal{J}\mathcal{J}^T)^{\ 1}$ denotes the pseudo inverse of $\mathcal{J}$, I is the identity matrix (q size), $\nabla\Phi$ is defined as the gradient of an objective function $\Phi(q)$ and α is the projection magnitude. This is constructed by aggregating the weighted criteria (Lee and Buss, 2006). It is defined by:

$$\Phi(q) = \sum_i^k w_i(\Phi_i(x))\Phi_i(q)$$
$$\text{with} \quad \Phi_i(q) = \frac{\Phi_i(q) \quad \Phi_{i\min}}{\Phi_{i\max} \quad \Phi_{i\min}} \tag{14}$$

$\Phi_i(q)$ is the normalized function which depends on the $\Phi_i(q)$ criteria, w_i is a trigonometric function to satisfy the boundary conditions of zero derivative limit values. Two thresholds are associated with each weighting function: a minimum threshold below which the test is considered critical ($w_i = 1$), and a maximum threshold below which the test is considered satisfactory ($w_i = 0$) (Guire *et al.*, 2010). $\Phi_i(x)$ is a weighting to define a dominance of the criteria face to the others as joint limits or singularity.

3.2 Optimization criteria

There are a multitude of criteria used to improve the behaviour of robotic applications (Merlet, 1997; Khalil and Dombre, 2002) each of which has been developed in a context and for a purpose. We first introduce the classical criteria such as the joint limits and wrist singularity defined by:

Table I Torque and speed of the human arm joints

Joint no.	Max torques (Nm)	Reference	Max. velocities (rad/s)	Reference
1	90	Fleisig *et al.* (1995)	4	
2	90	Fleisig *et al.* (1995), Debicki *et al.* (2010)	4	Debicki *et al.* (2010)
3	60		9	
4	40	Debicki *et al.* (2010), Guenzkofer *et al.* (2011)	12	Debicki *et al.* (2010)
5	16		17	
6	10	Lehman and Calhoun (1990)	21	Debicki *et al.* (2010)

$$\Phi_j(q) = \sum_{i\ 1}^{n} \left[\frac{q_i \quad q_{imoy}}{\Delta q_i} \right]^2 \tag{15}$$

$$\text{with } \Delta q = q_{\max} \quad q_{\min} \text{ and } q_{moy} = \frac{1}{2}(q_{\min} + q_{\max})$$

$$\Phi_s(q) = \|q \quad q_s\| \text{ where } q_s \text{ represents the wrist singularity configuration } (q_5 = 0) \tag{16}$$

We also introduce criteria related to process constraints such as the α cutting angle defined by Φ_α and $\Phi_r(q)$, a criterion of stiffness capacity defined by:

$$\Phi_\alpha = \|\vec{F}_c \vec{u}_6\| \text{ with } \vec{u}_6 \text{ the rotation axis of the end effector :} \tag{17}$$

$$\Phi_r(q) = \sum_{i\ 2}^{3} q_i \text{ with } q_i \text{ the articular value of } q_2 \text{ and } q_3. \tag{18}$$

Compared to the specificities of the cutting strategy, we also introduce two criteria related to the dexterity and the mechanical performance previously defined. The local optimization (equation (13)) integrates a modification of the configuration by adding a variation of the positioning of each actuator at each trajectory point by:

$$q_i = q_i + dq_i \text{ with } dq_i = \alpha(I \quad \mathcal{J}^+\mathcal{J}) \sum_{1}^{n} w_i \Phi_i(x) \nabla \Phi_i(q) \tag{19}$$

We present the algorithm structure in Figure 5.

3.3 Setting thresholds

Our method requires the definition of Φ_{imin} and Φ_{imax} for each criterion (Figure 6). In the case of criteria Φ_s (singularity) and Φ_j (joint limits), the minimum threshold is set between 10 and 20 per cent of the limit value to ensure the consideration of the variability of real trajectories. For the other criteria, we study the variations of two optimization variables α and q_7 for $\alpha \in [0, 90°]$ and $q_7 \in [\ 50°, 50°]$ around the position of the fat vein. A value of the criteria is only given when the inverse geometric model (IGM) return a feasible configuration away of joint limits. The position marked in thin line is the value of the wrist singularity q_s corresponding to $q_7 = 5°$. In this configuration, the cutting plane P_c (Figure 3) is aligned with the plane including the axis of q_1 and q_4. Because we want to maximize all of the criteria for all poses of the trajectory, we consider the search space to the left of the q_s singular position. It is now positioning the minimum and maximum thresholds for each criterion to ensure that the search space during the optimization is large enough to take into account all the criteria. In the case of AB cutting, we seek to ensure good mechanical behaviour of the ratio whose highest values r_{md} lie in the interval $q_7 \in [\ 50°, \ 20°]$ (Figure 6). This sets the maximum threshold criterion of r_{md} without restricting consideration for other criteria. Thus, the first threshold of Φ_α is set to 55°, a value beyond which the criterion is not taken into account and the second threshold is set to 70°, the value below which the cutting process is highly degraded. This also allows us to set thresholds for the other two criteria Φ_r and $r_{vd.}$.

4. Application in two specific cuttings in deboning

Applications are dedicated to AB cutting and BC cutting. The procedure is deeply presented in the case of the second

Figure 5 Path planning optimization

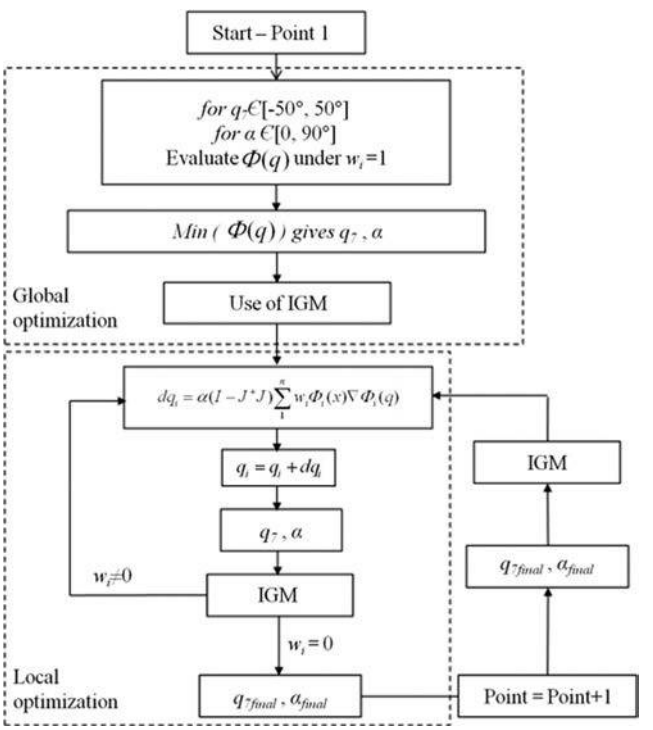

Figure 6 Criteria variation in the workspace for AB cutting to adjust the weighting

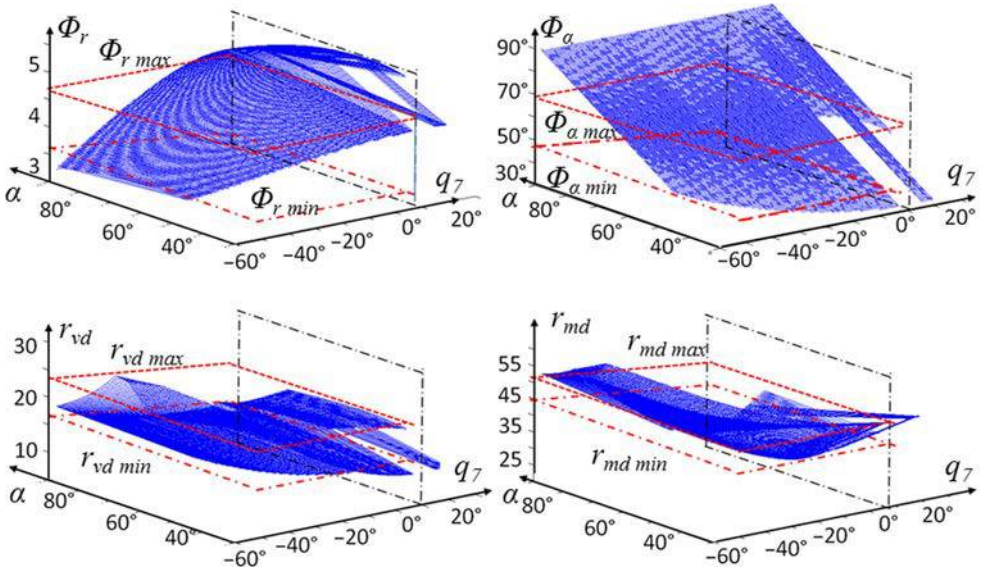

fat vein and results are presented for the BC cutting. The optimization performed in Matlab® generates RAPID code language. When the optimized path corresponds to our expectations, it is synchronized directly with the real robotic cell for evaluating the cutting process.

4.1 Cutting along the second fat vein

The scenario of the cut along the second fat vein (Figure 7) show that the displacement is mainly located along joints two, four and six associated with θ_{21}, θ_{43} and θ_{65} (Figure 8). The gesture analysis shows that the operator from position 3 minimizes torque induced on his wrist by aligning it with his forearm ($\theta_{65} \approx 0°$). The cutting plane P_c (Figure 3) is thus aligned with the plane defined by the P_{arm} arm and forearm itself vertically aligned ($\theta_{10} \approx 0°$) that allows the operator to generate huge forces (> 100 N). The optimization tools and simulation are implemented in Matlab® (Figure 9). The reorientation of the arm around θ_{tool} causes alignment of the P_{arm} plan, defined by the arm and forearm with the cutting plan P_c. This configuration is linked to a global increase of the r_{md} ratio (Figure 10(b)). The torque minimization on joint five and six with a wrist value close to 0° corresponds to a maximized torque on joint two and four (Figure 10(a)). This posture highlights the fact that the criterion of mechanical performance have to be used (Figure 10(b)). Now, if we compare the curves for different optimized path, Figure 11(a) and (c) with curves Figure 11(b),

Figure 7 Scenario of the cut along the second fat vein segmented in eight sequential motions

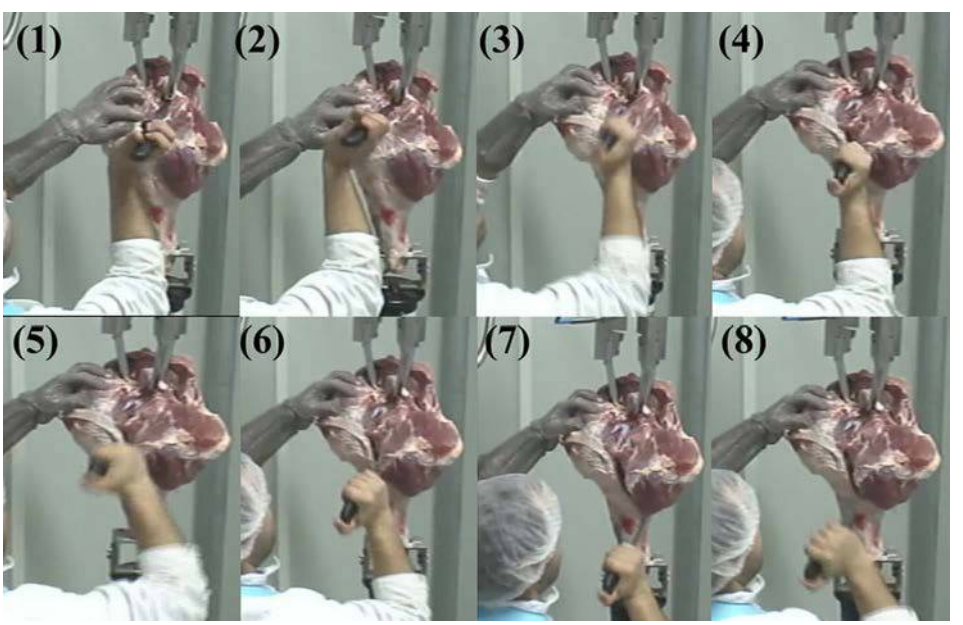

Figure 8 Evolution of the medium values of joint angle values during the cut of the second fat vein for various time period

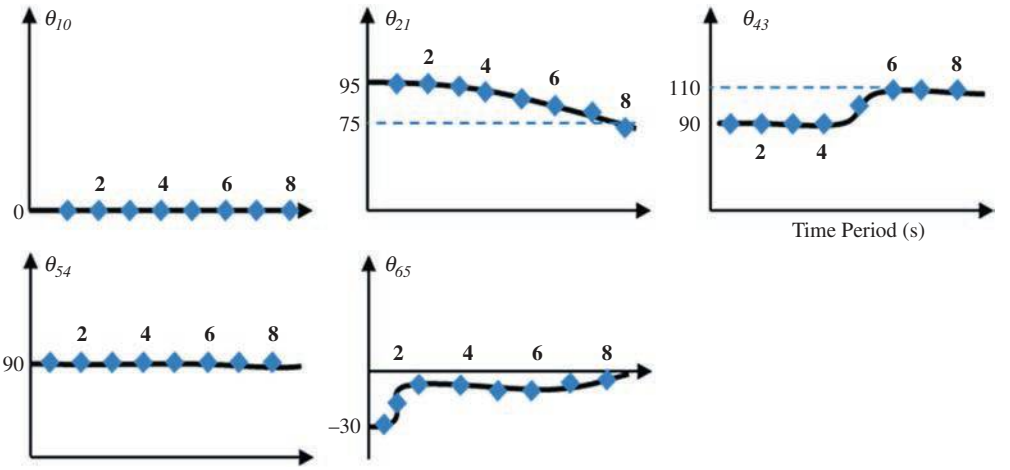

Figure 9 (a) Model reorientation around θ_{tool} from $\theta_{tool} = 0°$ to $\theta_{tool} = 90°$, (b) model reorientation around $\theta_{shoulder}$ (to 0° to 90°) and θ_{tool}

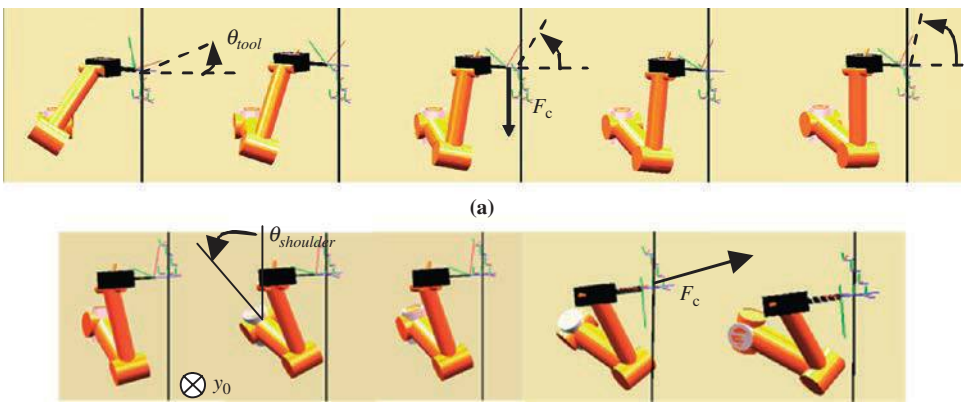

a sharp increase in r_{md} and Φ_r criteria highlights the criteria choice. This behaviour shows a great improvement in the working conditions of the cell. There is also a small improvement in Φ_α criterion where the reorientation of the blade in cutting plane P_c is severely limited by the articular joint limit q_3 for this trajectory (Figure 11(a) and (c)). The study of these curves shows the importance of criteria weighting on the results of the optimization. In our case, the selected solution is one of Figure 11(c) which has the better performances for Φ_α criteria. The results showing the cutting process on a ham with the robotic cell are presented in Figure 15(a) and (b).

4.2 Cuts around the kneecap

The gesture analysis (Figure 12) shows that the operator from position 2 realizes a contortion of his body to be well positioned to move closer to the alignment of planes P_{arm} and P_c for the forces transmission. In position 4, the wrist reaches his articular limits and speed has to be transmitted to the knife to cuts around the kneecap. It corresponds in position 3 and 4 to a repositioning of the butcher. Between position 5 and 6, the difficulty he has to transmit cutting force lead to the transmission of a V_n normal speed to perform the task. The simulation (Figure 9(b)) of the distorsion of the butcher includes two steps. The first one corresponds to a reorientation around $\theta_{shoulder}$ and the second one is a reorientation around θ_{tool} to reach $\theta_{65} \approx 70°$ when $\theta_{shoulder} > 60°$. The simulation of the actuated torque highlights a decrease of joint torque five (Figure 13(a)). The Table I shows that the maximal torque for this joint is 16 Nm. The movement could not be realized due to the mechanical performance of the human arm. This distortion around θ_{tool} is a way to improve the mechanical performance at the expense of kinematic performance (Figure 13). The analysis of the operator's gestures showed the dexterity criterion has to be preferred while considering the torque ratio to be greater than 1. The curves in Figure 14 show the behaviour improvement while having a decrease and an increase of criteria. We may note that, for this trajectory without optimization, the manipulator reaches the end of the trajectory close to the q_5 joint limit (130°) with critical Φ_α and Φ_r (Figure 14(a)). The decrease of the r_{vd} ratio leads to an increase of Φ_α and Φ_r criteria. So, the achieved optimization better improves the overall behaviour. The results while realizing the kneecap trimming are presented in Figure 15(c) and (d).

Figure 10 (a) Joint torques depending on θ_{tool}, (b) evaluation of the force and speed criteria for a force of 50 N and a speed of 50 mm/s, (c) evolution of dexterity criteria and mechanical criteria

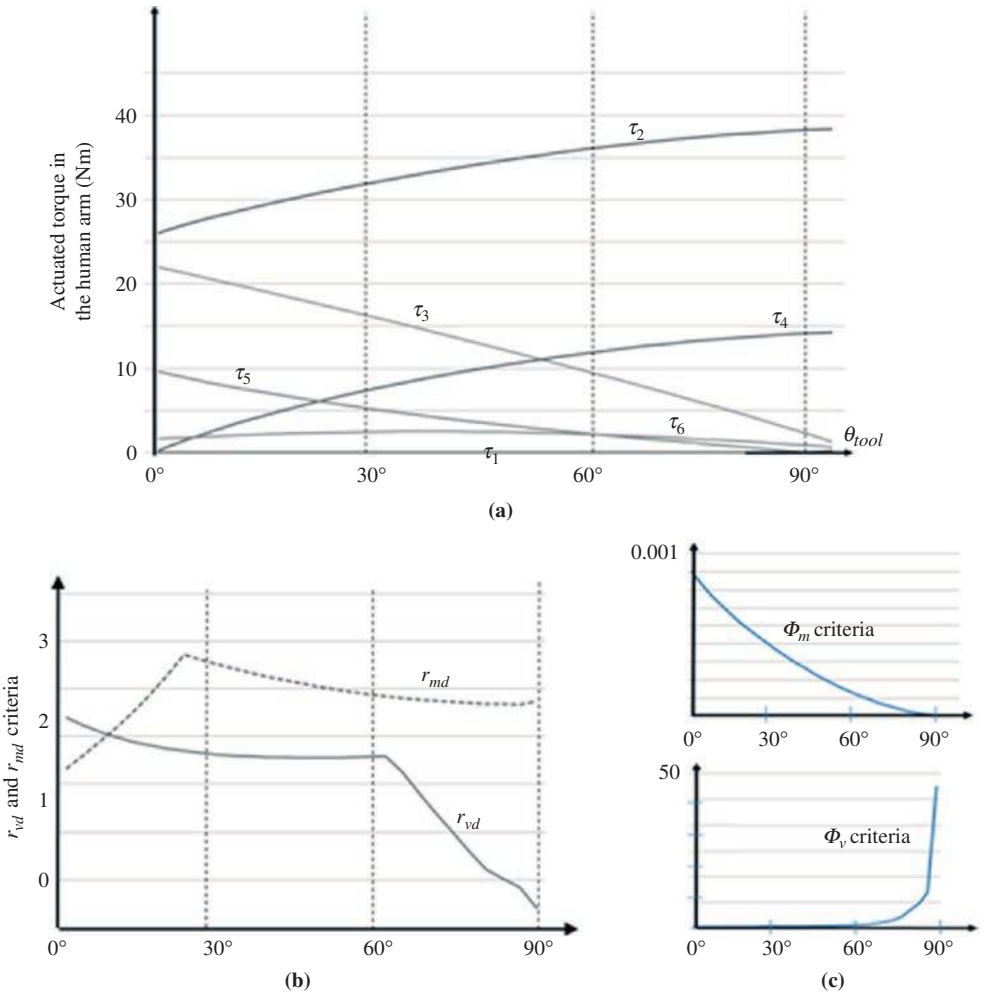

Figure 11 Evaluation of normalized criteria when two are considered in the optimization

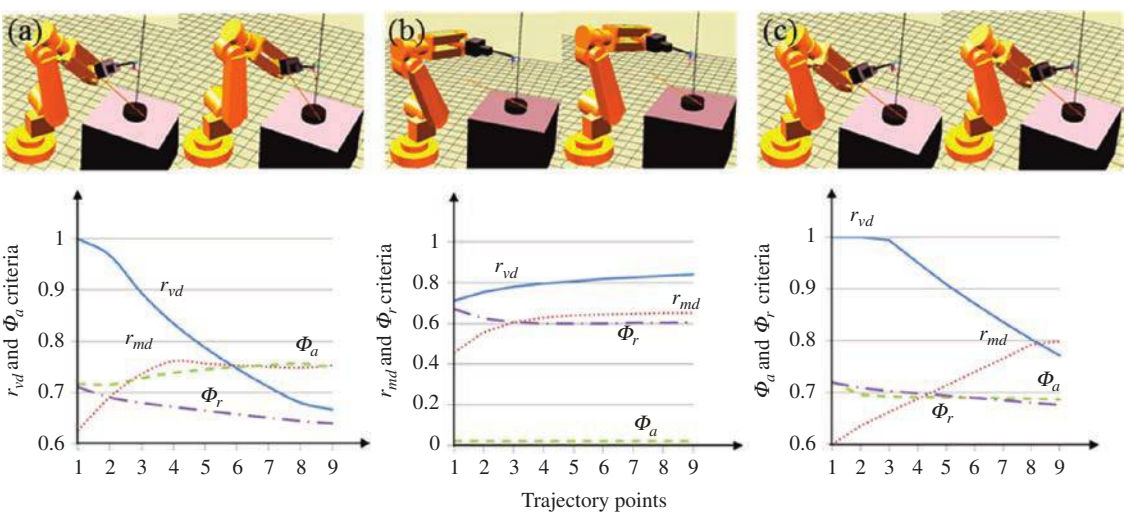

Figure 12 Scenario for the cuts around the kneecap

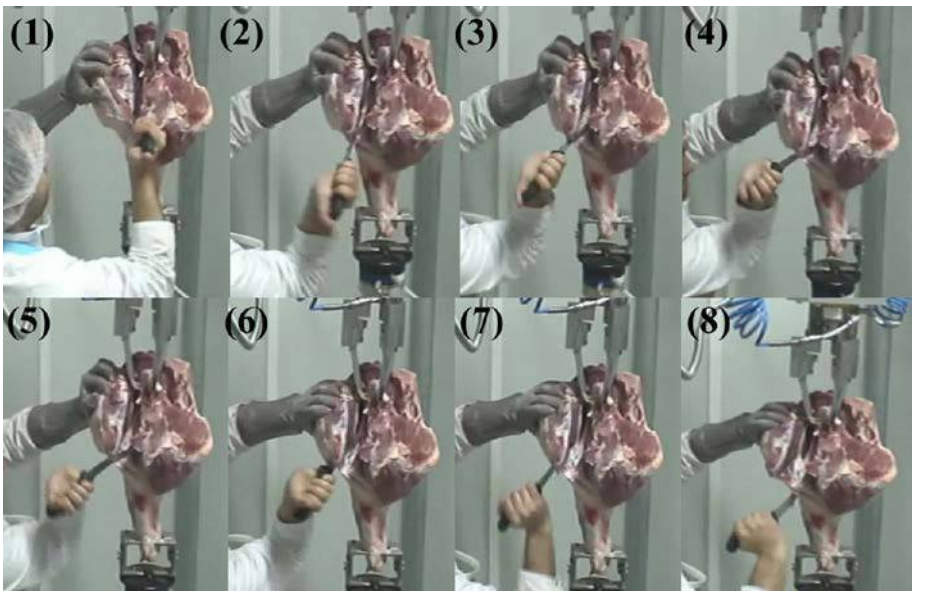

Figure 13 Articular torque and evaluation of Φ_v and Φ_m for a force of 50 N and a speed of 50 mm/s

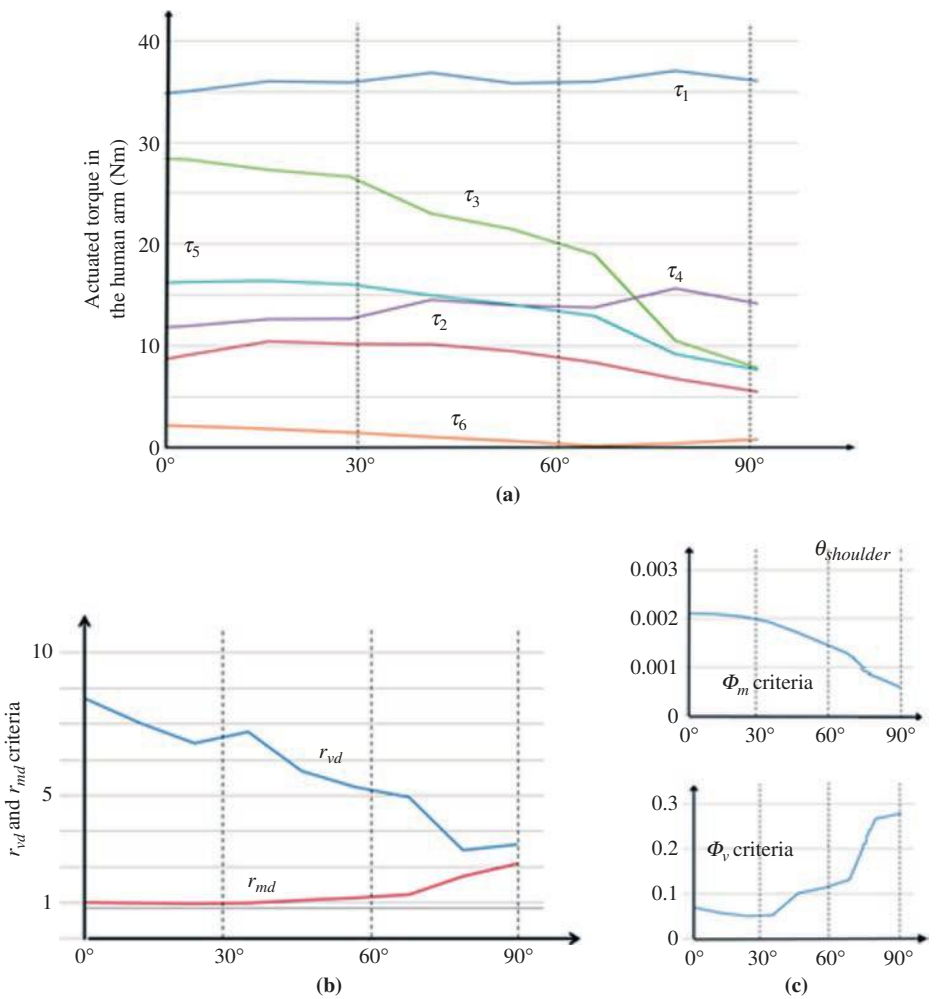

Figure 14 (a) Non optimized cutting path, (b) optimized cutting path for the cuts around the kneecap

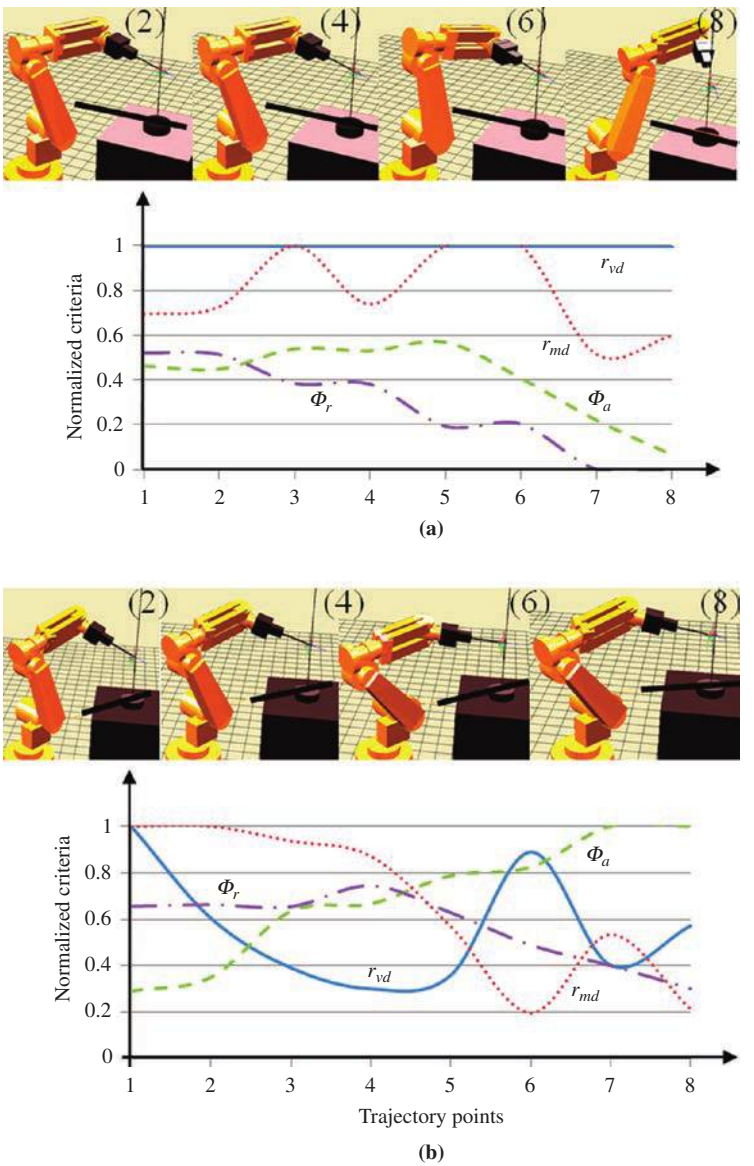

5. Conclusion

The work presented in this paper concerns the improvement of the robotized cutting process based on the human arm analysis. We present the cutting strategy based on the use of an industrial force control for opening muscles along the bone and setting parameters to ensure the cutting process. The proposed path planning with a seven DoFs redundant robotic cell requires criteria implementation. The method of redundancy resolution is based on a multicriteria optimization. We present two criteria specifically related to dexterity and mechanical performance. First, we evaluate the effectiveness of these criteria with a human arm model by comparing the results with respect to the gestures of the butcher. These criteria are then applied to plan optimized paths in a redundant robotic cell. The choice of thresholds for the different criteria and weighting adjustment are presented. The weighting way to adjust the search solution based on the specificity of the task highlights the usefulness of the presented method.

Figure 15 (a) Robotized deboning along the second fat vein, (b) results of the cutting of the second fat vein, (c) cuts around the kneecap, (d) results

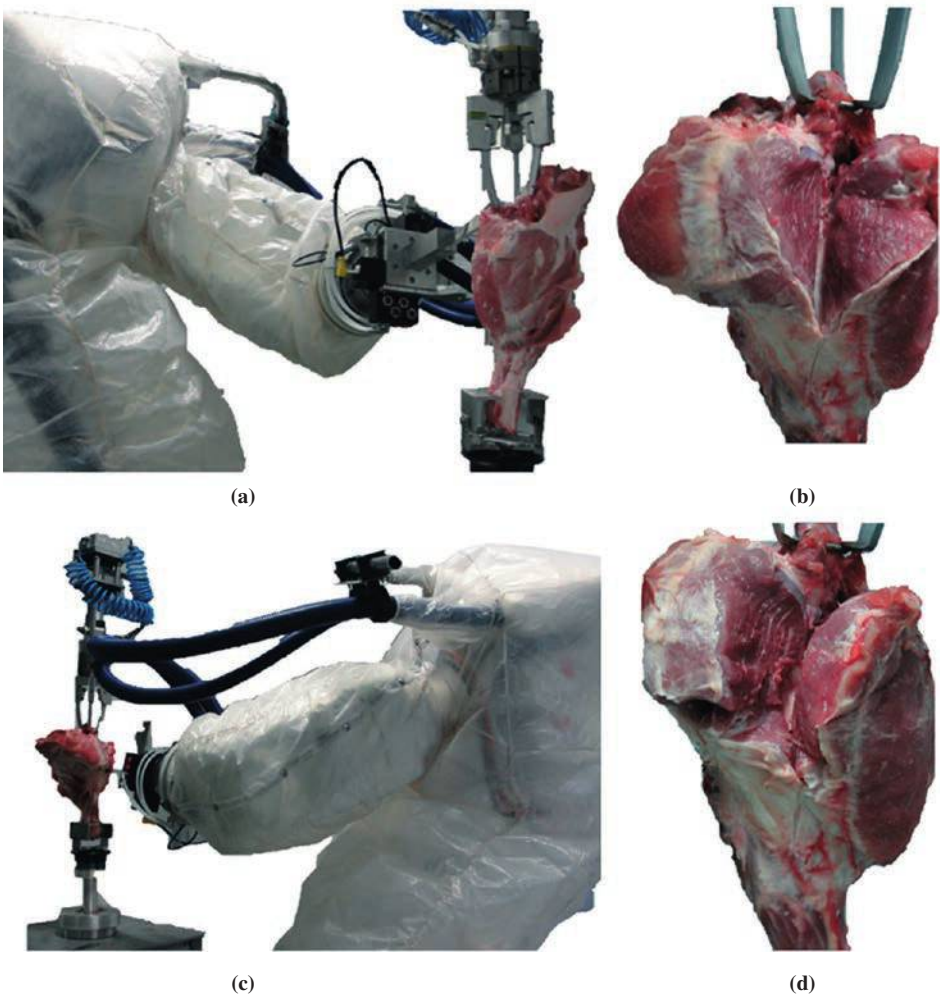

References

ABB (2005), *Application Manual for Force Control for Machining*, available at: www.trinisoft.at/files/3HAC027595 001 revH en.pdf (accessed July 4, 2013).

Aimers, R.J., Arnold, A.R. and Le Masurier, R.G. (2003), "Animal carcass leg removal method and apparatus", International Publication No. WO2003096814.

Artemiadis, P.K., Katsiaris, P.T. and Kyriakopoulos, K.J. (2010a), "A biomimetic approach to inverse kinematics for a redundant robot arm", *Autonomous Robots*, Vol. 9 Nos 3/4, pp. 293 308.

Artemiadis, P.K., Katsiaris, P.T., Liarokapis, M.V. and Kyriakopoulos, K.J. (2010b), "Human arm impedance: characterization and modeling in 3D space", *Proc. IEEE/RSJ Int. Conf. on Intelligent Robots and Systems*, pp. 3103 3108.

Campos, F.M.M.O. and Calado, J.M.F. (2009), "Approaches to human arm movement control a review", *Annual Reviews in Control*, Vol. 33 No. 1, pp. 69 77.

CNAMTS (2004), *Statistiques nationales des accidents du travail, des accidents de trajet et des maladies professionnelles Année 2002*, Caisse Nationale d'Assurance Maladie des Travailleurs salariés, Paris.

Debicki, D.B., Watts, S., Gribble, P.L. and Hore, J. (2010), "A novel shoulder elbow mechanism for increasing speed in a multijoint arm movement", *Experimental Brain Research*, Vol. 203 No. 3, pp. 601 613.

Dubey, R. and Luh, J. (1988), "Redundant robot control using task based performance measures", *Journal of Robotic Systems*, Vol. 5 No. 5, pp. 409 432.

Fleisig, G.S., Andrews, J.R. and Dillman, C.J. (1995), "Kinetics of baseball pitching with implications about injury mechanisms", *The American Journal of Sports Medicine*, Vol. 23 No. 2, pp. 233 239.

Gogu, G., Coiffet, P. and Barraco, A. (1997), *Représentation des déplacements finis et infinitésimaux des robots*, Edition Hermès, Paris.

Gomi, H. and Kawato, M. (1997), "Human arm stiffness and equilibrium point trajectory during multi joint movement", *Biological Cybernetics*, Vol. 76 No. 3, pp. 163 171.

Guenzkofer, F., Engstler, F. and Bubb, H. (2011), "Isometric elbow flexion and extension joint torque measurements considering biomechanical aspects", *First International Symposium on Digital Human Modeling*, pp. 14 15.

Guire, G., Sabourin, L., Gogu, G. and Lemoine, E. (2010), "Robotic cell for beef carcass primal cutting and pork ham boning in meat industry", *Industrial Robot: An International Journal*, Vol. 37 No. 6, pp. 532 541.

Hamdas (2010), available at: www.mayekawausa.com/products/robotics/hamdasR.html (accessed April 17, 2013).

Hinrichsen, L. (2010), "Manufacturing technology in the Danish pig slaughter industry", *Meat Science*, Vol. 84 No. 2, pp. 271 275.

James, S.J., Purnell, G. and James, C. (2009), *Forty Two Years of Food Process Engineering Research at Langford*, Food Refrigeration & Process Engineering Research Centre, University of Bristol, Langford.

Khalil, W. and Dombre, E. (2002), *Modeling, Identification and Control of Robots*, Hermès Penton, London.

Kim, H., Li, Z., Milutinovic, D. and Rosen, J. (2012), "Resolving the redundancy of a seven DOF wearable robotic system based on kinematic and dynamic constraint", *IEEE Int. Conf. on. Robotics and Automation*, pp. 305 310.

Kusuda, Y. (2010), "The use of robots in the Japanese food industry", *Industrial Robot: An International Journal*, Vol. 37 No. 6, pp. 503 508.

Lee, K.K. and Buss, M. (2006), "Redundancy resolution with multiple criteria", *IEEE/RSJ Int. Conf. on Intelligent Robots and Systems*, pp. 598 603.

Lehman, S.L. and Calhoun, B.M. (1990), "An identified model for human wrist movements", *Experimental Brain Research*, Vol. 81 No. 1, pp. 199 208.

Liegeois, A. (1977), "Automatic supervisory control of the configuration and behaviour of multibody mechanisms", *IEEE Transactions on Systems, Man, and Cybernetics*, Vol. 7 No. 12, pp. 868 871.

Merlet, J.P. (1997), *Les Robots Parallèles*, Hermès, Paris.

Mussa Ivaldi, F.A., Hogan, N. and Bizzi, E. (1985), "Neural, mechanical, and geometric factors subserving arm posture in humans", *The Journal of Neuroscience*, Vol. 5 No. 10, pp. 2732 2743.

Perdereau, V. and Drouin, M. (1993), "A new scheme for hybrid force position control", *Robotica*, Vol. 11, pp. 453 464.